ULTRASONIC SCATTERING AND NONDESTRUCTIVE EVALUATION OF DEFECTS

S.K. Datta[1]

S.H. Shah[2]

CUMER-86-5 August 1986

Contract N00014-86-K-0280

[1]Department of Mechanical Engineering and
Cooperative Institute for Research in Environmental Sciences
University of Colorado, Boulder, CO 80309 U.S.A.

[2]Department of Civil Engineering
University of Manitoba, Winnipeg, Canada R3T 2N2

ULTRASONIC SCATTERING BY

PLANAR AND NON-PLANAR CRACKS

Subhendu K. Datta

Department of Mechanical Engineering
and Cooperative Institute
for Research in Environmental Sciences
University of Colorado
Boulder, CO 80309, U.S.A.

Arvind H. Shah

Department of Civil Engineering
University of Manitoba
Winnipeg, Canada R3T 2N2

INTRODUCTION

Problems of elastic wave scattering by surface-breaking and near-surface cracks are of considerable current interest for ultrasonic nondestructive evaluation. Ultrasonic scattering by planar cracks near or at the free surface of a semi-infinite elastic homogeneous medium has been studied theoretically by many authors. References to recent papers on this subejct can be found in [1], [2] and [3]. Some experimental works on surface-breaking normal planar cracks have also appeared ([4] - [6]).

Ultrasonic scattering by surface-breaking planar and branched cracks of arbitrary orientation is the subject of this investigation. To our knowledge this problem has not received much attention in the literature. An approximate solution that is valid at low frequencies was presented in [7] for SH wave diffraction by a canted surface-breaking planar crack. Subsequently, a hybrid finite element and eigenfunction technique was used in [8] to study SH wave diffraction by planar surface-breaking canted crack.

In this paper we use the same hybrid t chnique as in [8] to study the scattering of in-plane body and surface waves by canted planar and normal surface-breaking branched cracks. We focus our attention to the near-field. Numerical results are presented for the vertical surface displacement amplitudes near the base of the crack.

FORMULATION AND SOLUTION

Consider a homogeneous, isotropic, and linearly elastic medium with a near-surface inhomogeneity of arbitrary properties and shape as shown in Figure 1. Assume the displacement $u(x, y, t)$ at a point P to be time-harmonic of the form $u(x, y)e^{-i\omega t}$,

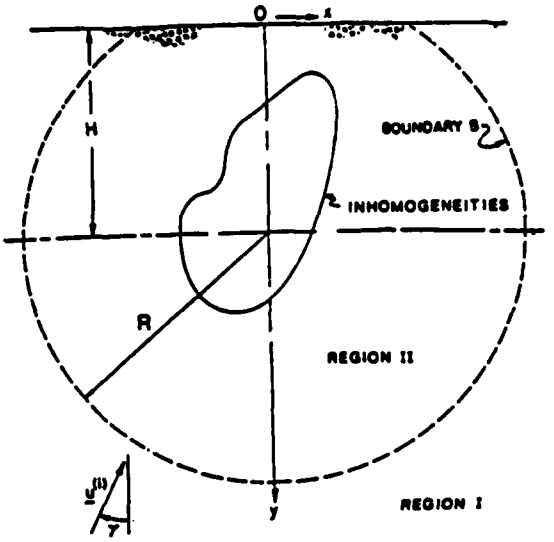

Fig. 1 Geometry of a near-surface inhomogeneity

where ω is the circular frequency. Then u satisfies the equation of motion in $y > 0$ (at points not on the crack)

$$\mu\nabla^2 u + (\lambda + \mu)\nabla\nabla \cdot u = -\rho\omega^2 u \tag{1}$$

where λ, μ are Lamé constants, ρ the mass density and the factor $e^{-i\omega t}$ has been dropped.

The solution of (1) can be expressed in terms of the longitudinal and shear wave potentials, ϕ and ψ, in the form

$$u = \nabla\phi + \nabla \times (\psi e_z) \tag{2}$$

Furthermore, in a homogeneous half-space, ϕ and ψ can be expressed in infinite series of multipolar potentials as [9],

$$\phi = \sum_{n=-\infty}^{\infty} (a_n \phi_n^p + b_n \phi_n^s)$$

$$\psi = \sum_{n=-\infty}^{\infty} (a_n \psi_n^p + b_n \psi_n^s) \tag{3}$$

where expressions for $\phi_n^p, \psi_n^p, \phi_n^s$ and ψ_n^s can be found in [9]. The coefficients a_n, b_n are found by satisfying the appropriate boundary conditions.

The representation (3) is not useful for satisfying the boundary conditions on the crack surface. For this reason, a different representation is needed in this near-field region. In this paper, the region inside the fictitious boundary B (Fig. 1) is divided into finite elements having N_I number of interior nodes and N_B number of boundary nodes.

For the finite element representation in region II, the energy functional is taken to be

$$F = \frac{1}{2}\int\int_{R_{II}} (\sigma \cdot \epsilon^* - \rho\omega^2 u \cdot u^*) dx dy - \frac{1}{2}\int_B (P_B \cdot u_B{}^* + P_B{}^* \cdot u_B) ds \tag{4}$$

where " * " indicates complex conjugate and σ and ϵ are column vectors defined as

$$\sigma = \{\sigma\} = (\sigma_{xx}, \sigma_{yy}, \sigma_{xy})^T \tag{5}$$

$$\epsilon = \{\epsilon\} = (\epsilon_{xx}, \epsilon_{yy}, \epsilon_{xy})^T \tag{6}$$

Superscript "T" denotes transpose. The P_B and U_B represent the traction and displacement on B, respectively.

It is assumed that the displacement field within the j^{th} element is represented in terms of the shape functions $L_j(x,y)$ and elemental nodal displacements $\{q_j^e\}$ as

$$u^e = \sum_{j=1}^{N_e} L_j q_j^e \tag{7}$$

where each q_j^e has two components u_{xj} and u_{yj} along the x and y directions, respectively. The N_e represents the number of nodes in each element.

The σ_{ij}^e and ϵ_{ij}^e are computed by substituting Eq. (7) into strain-displacement relations and these, in turn, into the stress-strain relations. Using these in Eq. (4), we get

$$F = q_I^{*T} S_{II} q_I + q_I^{*T} S_{IB} q_B + q_B^{*T} S_{BI} q_I$$
$$+ q_B^{*T} S_{BB} q_B - q_B^{*T} P_B^{(1)} - P_B^{*T(1)} q_B \tag{8}$$

in which $q_I = q_I{}^{(2)}, q_B = q_B{}^{(2)}, P_B{}^{(1)} = P_B{}^{(2)}$ and the elemental impedance matrices S_{ij} are defined as

$$[S^e] = \int\int_{R_e} ([B^e]^T [D][B^e] - \rho_e \omega^2 [L]^T [L]) dx dy. \tag{9}$$

In Eq. (9),

$$[B^e] = \begin{bmatrix} \frac{\partial}{\partial x} & 0 \\ 0 & \frac{\partial}{\partial y} \\ \frac{\partial}{\partial y} & \frac{\partial}{\partial x} \end{bmatrix} \begin{bmatrix} L_1 & 0 & L_2 & .. \\ 0 & L_1 & 0 & .. \end{bmatrix} = [N][L].$$

Note that [L] is a 2 x $2N_e$ matrix.

For an isotropic material [D] is given by

$$[D] = \begin{bmatrix} \lambda_e + 2\mu_e & \lambda_e & 0 \\ \lambda_e & \lambda_e + 2\mu_e & 0 \\ 0 & 0 & \mu_e \end{bmatrix}$$

where λ_e and μ_e are the Lamé's constant.

To find the constants a_n, b_n appearing in (3) and the nodal displacements in region II, it is necessary to use the continuity of displacement and traction on B. This is discussed in the following.

The incident displacement fields will be assumed to arise from the incident plane P and SV waves, and their reflections from the free surface $y = 0$. The case of incident Rayleigh waves will also be considered.

Let us suppose that in the absence of the crack the free field is the sum of the incident and reflected fields, that is

$$u_j^{(0)} = u_j^{(i)} + u_j^{(r)} \qquad (j = 1, 2). \tag{10}$$

For the Rayleigh wave $u_j^{(0)}$ is the associated displacement.

The total field outside B then is

$$u_j = u_j^{(S)} + u_j^{(0)} \qquad (j = 1, 2). \tag{11}$$

where $u_j^{(S)}$ is given by (2) and (3).

Using (2) and (3), the displacements at the nodes on B can be written as

$$\{q_B^{(S)}\} = [G]\{a\} \tag{12}$$

where [G] is a $2N_B$ x $2N_B$ matrix formulated in [10] and vector $\{a\}$ is

$$\{a\} = [a_1, ..., a_{N_B}, b_1, ..., b_{N_B}]^T$$

Similarly, using (2) and (3) in the stress strain relation, the traction at the nodes on B can be expressed in the form

$$\{\sigma_B^{(S)}\} = [F]\{a\} \tag{13}$$

where $[F]$ is also a $2N_B$ x $2N_B$ matrix defined in [10].

To express $\{\sigma_B^{(S)}\}$ in terms of $\{q_B^{(S)}\}$, we use the expression for the virtual work done on the boundary B, which is

$$\delta\pi = \int_B \{\delta q^*{}_B^{(1)}\}^T \{\sigma_B{}^{(1)}\} d\Gamma \tag{14}$$

where superscript (1) denotes the total field in region I (outside B).

Because of the continuity of displacements and traction on B, we have

$$q_B^{(1)} = q_B^{(2)} = q_B^{(0)} + q_B^{(S)} \tag{15}$$

$$\sigma_B^{(1)} = \sigma_B^{(2)} = \sigma_B^{(0)} + \sigma_B^{(S)} \tag{16}$$

where superscript (2) denotes the total field in region II.

Substituting (12), (13), (15), and (16) in Eq. (14), and noting that $\delta q_B^{(1)} = \delta q_B^{(S)}$, we obtain from eq. (14)

$$\delta\pi = \{\delta a^*\}^T \{P_B^{(1)}\} \tag{17}$$

where $P_B^{(1)}$ is given by

$$\{P_B^{(1)}\} = [\bar{R}]\{a\} + \{P_B^{(0)}\} \tag{18}$$

Here

$$[\bar{R}] = \int_B [G^*]^T [F] d\Gamma \tag{19}$$

and

$$\{P_B^{(0)}\} = \int_B [G^*]^T \{\sigma_B^{(0)}\} d\Gamma. \tag{20}$$

Substituting Eq. (12) into Eq. (8) and taking the variation, we obtain a set of simultaneous equations which may be written in matrix form as

$$\begin{bmatrix} S_{II} & S_{IB}G_I \\ G^{*T}S_{IB}^T & G^{*T}S_{BB}^G \end{bmatrix} \begin{bmatrix} q_I \\ a \end{bmatrix} = \begin{bmatrix} -S_{IB}q_B^{(0)} \\ -G^{*T}S_{BB}q_B^{(0)} + P_B^{(0)} \end{bmatrix}. \tag{21}$$

Using Eqs. (18) and (21), we obtain

$$[G^{*T}(S_{BB} - S_{IB}^T S_{II}^{-1} S_{IB} G^* - \bar{R}]\{a\} =$$

$$-G^{*T}(S_{BB} - S_{IB}^T S_{II}^{-1} S_{IB}) q_B^{(0)} + P_B^{(0)} \tag{22}$$

In Eq. (22), the generalized coordinates $\{a\}$ are the only unknowns. Therefore, $\{a\}$ can be evaluated. Once $\{a\}$ are known, the near and far displacement and stress fields can be determined.

NUMERICAL RESULTS AND DISCUSSION

In this paper, the boundary B enclosing the interior region is not a complete circle, and so the potentials ϕ_n^p, ψ_n^p, and ϕ_n^s, ψ_n^s cannot be expanded in cylindrical wave functions as was done in [1]. So the integrals giving these potentials and their derivatives were evaluated numerically for every node on B. The details are discussed in [11].

The hybrid method is employed to study scattering by P, SV and Rayleigh waves by three types of surface breaking cracks: a vertical crack (Fig. 2 with $\alpha = 90°$), a 45° inclined crack (Fig. 2 with $\alpha = 45°$), and a vertical branched (Y) crack (Fig. 3).

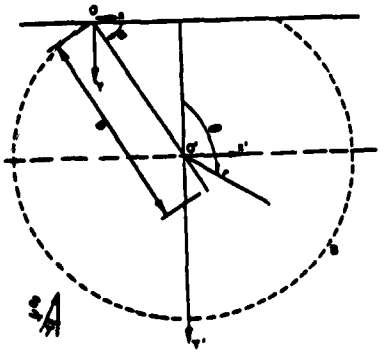

Fig. 2. Geometry of a planar crack

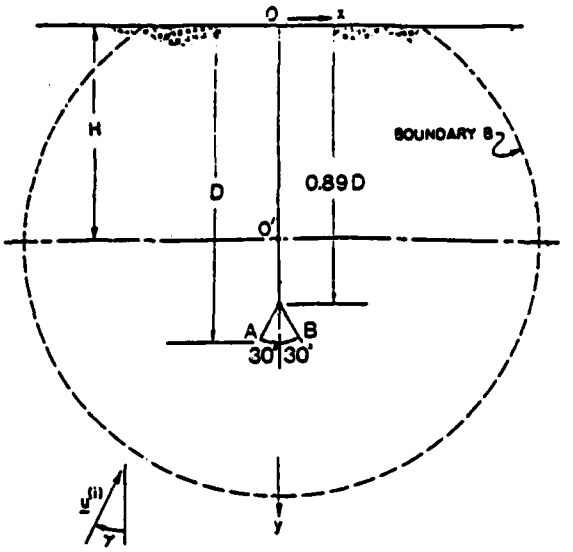

Fig. 3. A branched crack

Stress intensity factors at the tips of the cracks were calculated and for the particular case of a planar surface-breaking normal crack they were found to agree well with the results of [12].

The surface displacements at $y = 0$ are calculated by using (3) in (2) after $\{a\}$ are calculated. Normalized values of $u_y^{(S)}$ are presented in Figures 4-8. For each type of crack mentioned above five cases of incident waves were considered: plane P wave incident at 0° and 45°, plane SV wave incident at 0° and 45°, and finally Rayleigh wave. Some representative results are shown here.

Figures 4 and 5 show the scattered vertical surface displacement amplitudes for a Rayleigh wave incident from the left on a normal planar and branched crack. It is seen that there are large differences in the forward direction between the two cases as the frequency becomes large. In the backward direction, however, the differences are not very significant. Figures 6 and 7 show the results for an incident SV wave moving vertically as well as at 45° to the vertical. Large differences are found for vertical incidence, but not in the other case. Finally, in Figure 8 is shown the case of a Rayleigh wave incident on a canted crack. This figure is to be contrasted with Fig. 4. The large contrast shown clearly distinguishes a canted crack from a normal crack.

CONCLUSION

Model calculations of elastic wave scattering by surface-breaking planar and non-planar cracks have been presented. These calculations show that near-field surface displacements due to scattering by planar and branched cracks are quite different even when the branches are small. Also, it is found that signatures of normal and canted cracks are very dissimilar. These characteristic differences can be used to discriminate between the various cases.

Although the results presented here are for homogeneous medium, the technique can be generalized to study cracks in a composite medium. These are presently under investigation and will be reported later.

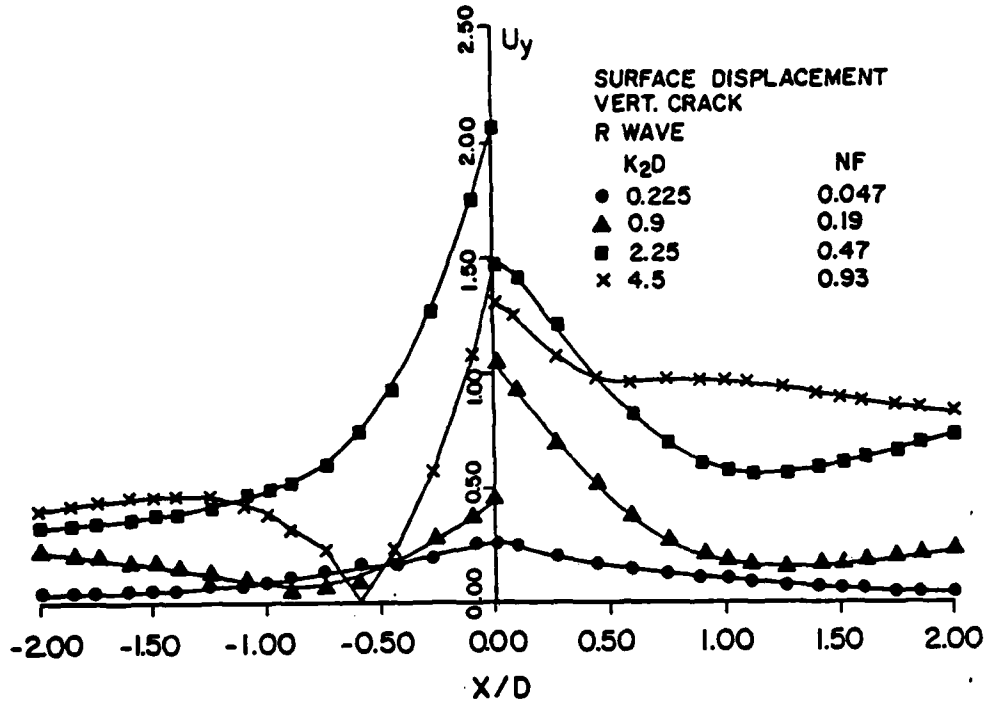

Fig. 4. Scattered vertical surface displacement amplitude due to normal planar crack

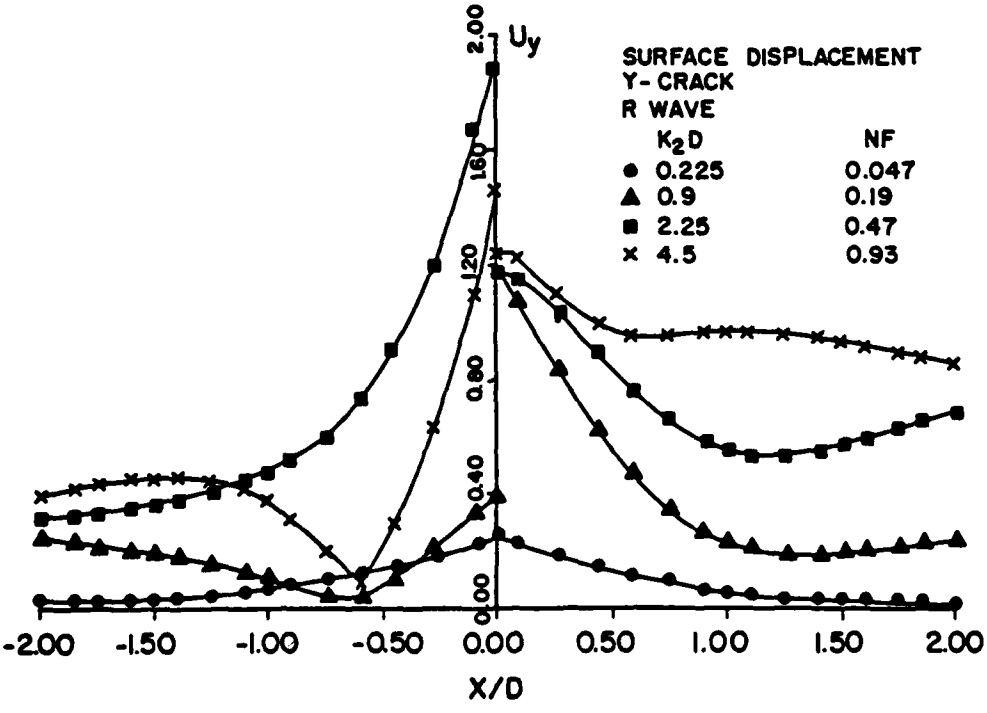

Fig. 5. Scattered vertical surface displacement amplitude due to normal branched crack

ACKNOWLEDGEMENT

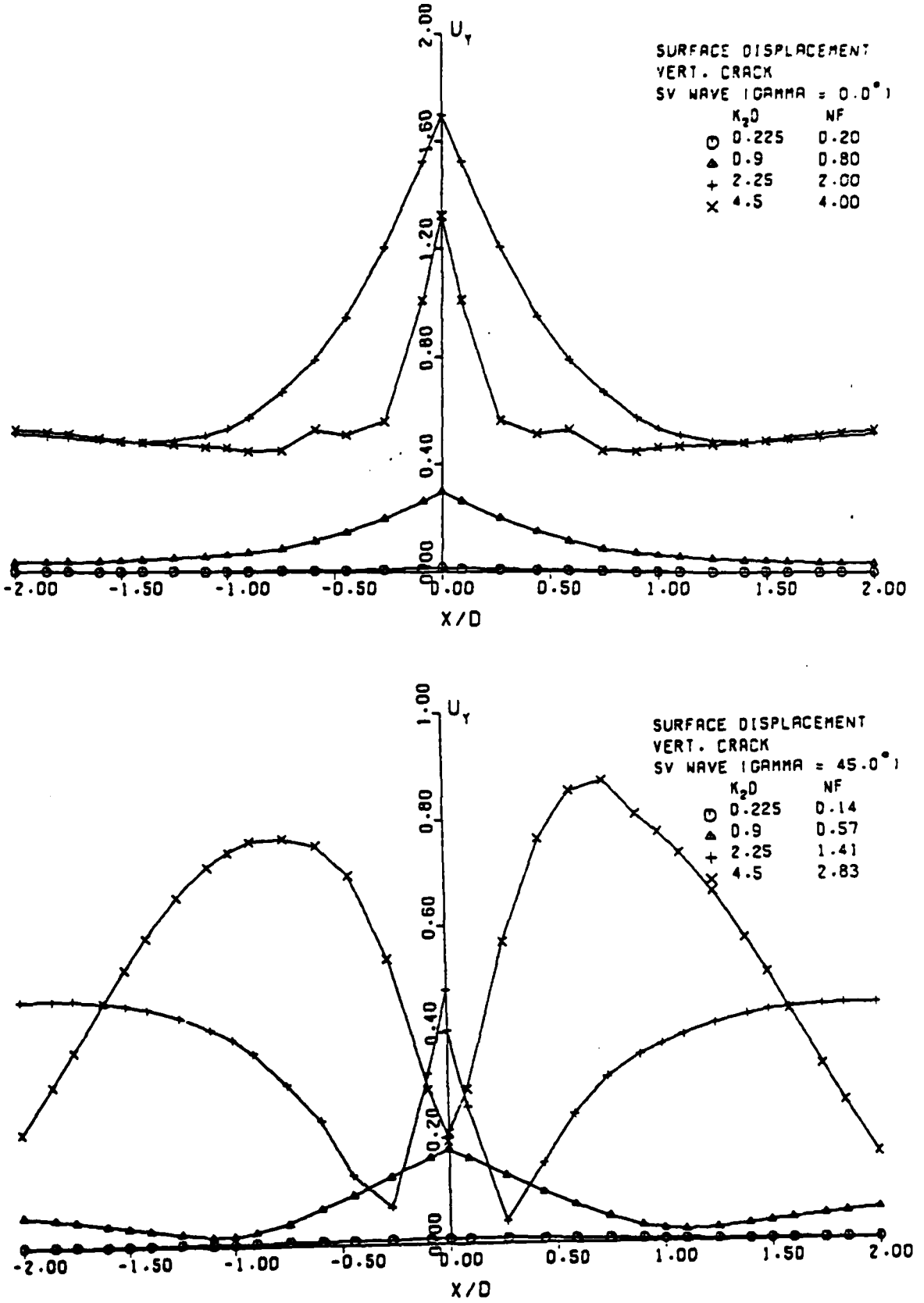

Fig. 6. Scattered vertical surface displacement due to vertical crack for incident SV waves

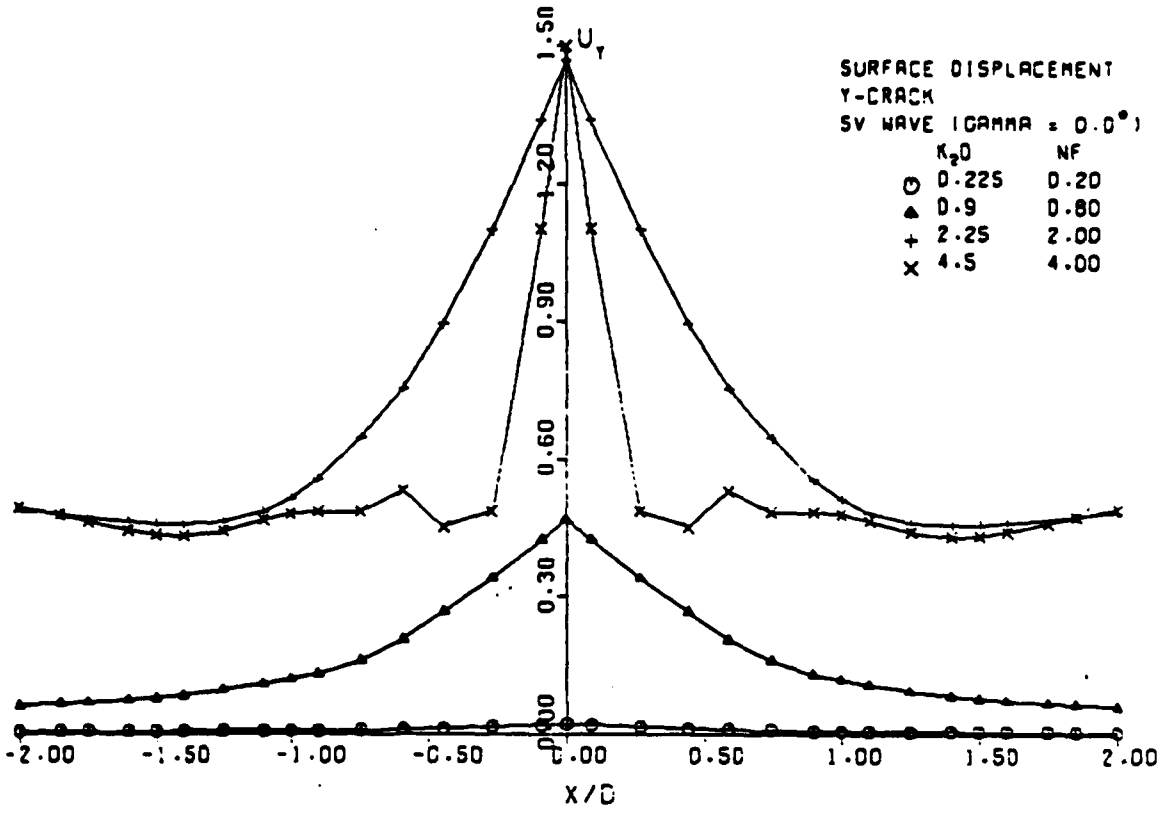

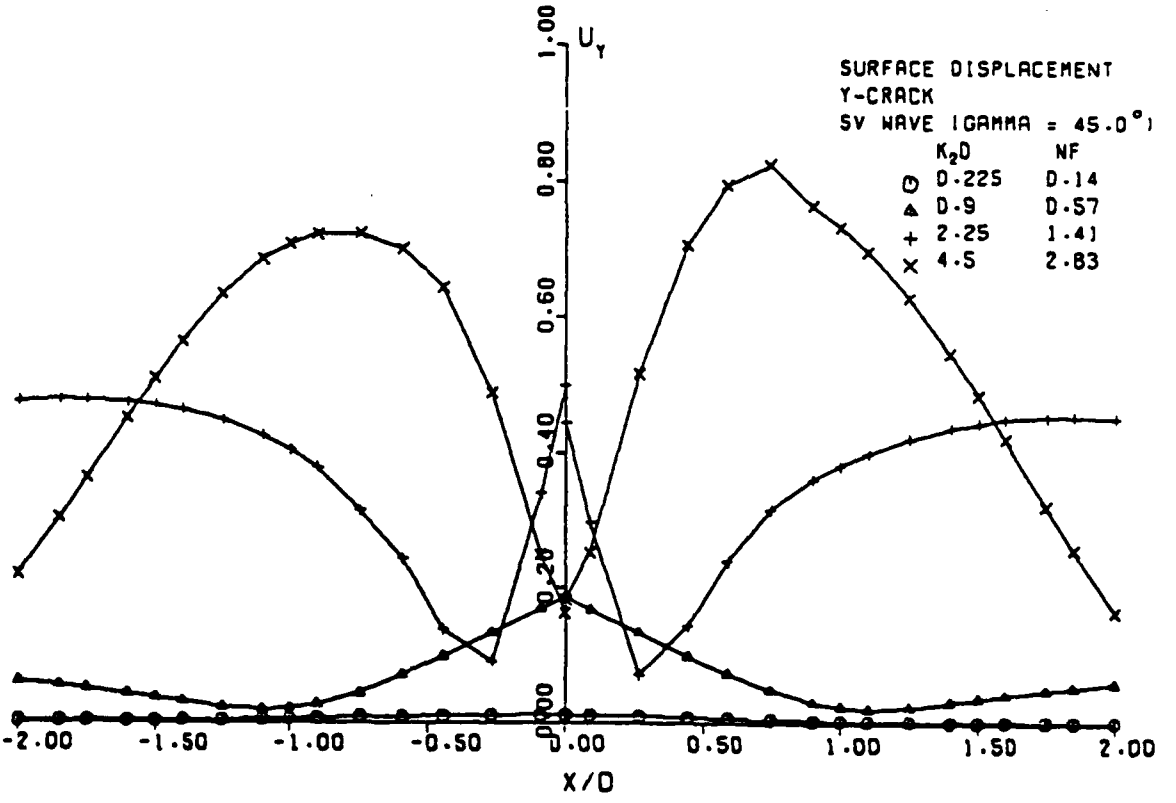

Fig. 7. Scattered vertical surface displacement due to Y crack for incident SV waves

Results presented here were partly supported by grants from the Office of Naval Research (N00014-86-K-0280), the National Science Foundation (CEE81-20536) and the Natural Science and Engineering Research Council of Canada (A-7988).

REFERENCES

1. A.H. Shah, K.C. Wong and S.K. Datta, Wave Motion *7*, 319 (1985).
2. J.D. Achenbach, Y.C. Angel and W. Lin, *in*: "Wave Propagation in Homogeneous Media and Ultrasonic Nondestructive Evaluation," G.C. Johnson, ed., American Society of Mechanical Engineers, New York (1984).
3. J.H.M.T. van der Hijden and F.L. Neerhoff, J. Acoust. Soc. Am. *75*, 1694 (1984).
4. M. Hirao, H. Fukuoka and Y. Miura, J. Acoust. Soc. Am. *72*, 602 (1982).
5. C.H. Yew, K.G. Chen and D.L. Wang, J. Acoust. Soc. Am. *75*, 189 (1984).
6. R. Dong and L. Adler, J. Acoust. Soc. Am. *76*, 1761 (1984).
7. S.K. Datta, J. Appl. Mech. *46*, 101 (1979).
8. S.K. Datta, A.H. Shah and C.M. Fortunko, J. Appl. Phys. *53*, 2895 (1982).
9. S.K. Datta and N. El-Akily, J. Acoust. Soc. Am. *64*, 1692 (1978).
10. A.H. Shah, Y.F. Chin and S.K. Datta, to be published.
11. Y.F. Chin, "Scattering of Elastic Waves by Near-Surface Inhomogeneities," M.S. Thesis, Department of Civil Engineering, University of Manitoba (1985).
12. J.D. Achenbach, L.M. Keer and D.A. Mendelsohn, J. Appl. Mech. *47*, 551 (1980).

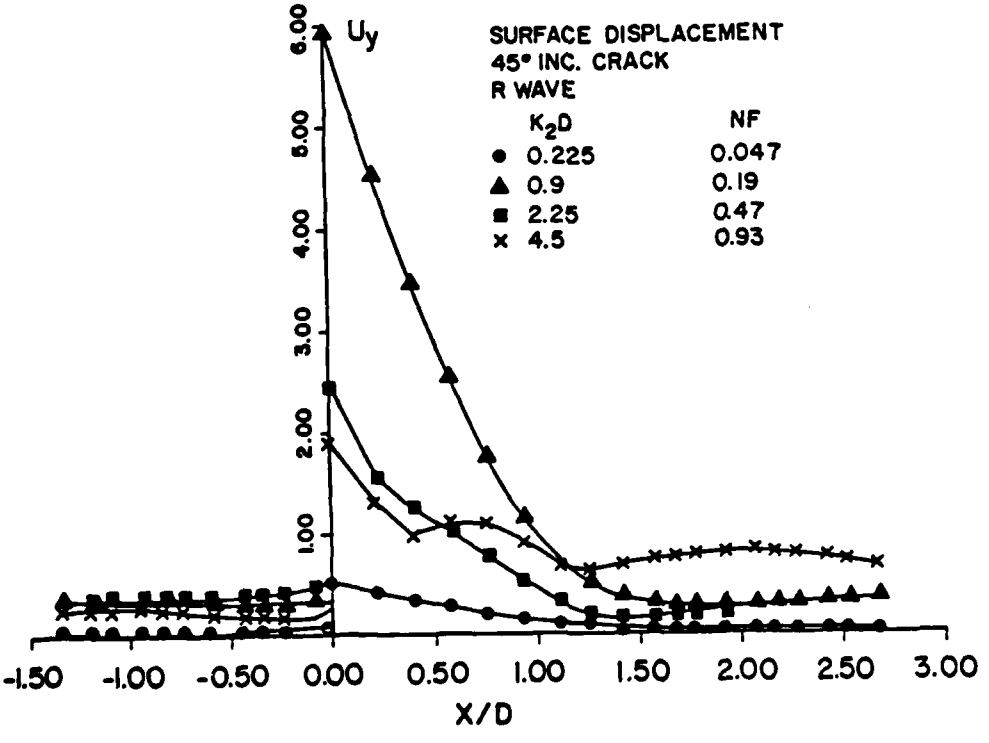

Fig. 8. Scattered vertical surface displacement due to 45° inclined crack for incident R wave